Acta Geochim (2021) 40(6):961–972
https://doi.org/10.1007/s11631-021-00492-0

ORIGINAL ARTICLE

Distribution of functional microorganisms and its significance for iron, sulphur, and nitrogen cycles in reservoir sediments

Shuang Bai[1] · Meilin Yang[1] · Zheng Chen[2] · Ming Yang[1] · Jing Ma[1] · Xue-Ping Chen[1] · Fushun Wang[1]

Received: 5 July 2021 / Revised: 2 August 2021 / Accepted: 6 August 2021 / Published online: 9 September 2021

Abstract The biogeochemical cycles of sulphur (S), iron (Fe) and nitrogen (N) elements play a key role in the reservoir ecosystem. However, the spatial positioning and interrelationship of S, Fe and N cycles in the reservoir sediment profile have not been explored to a greater extent. Here, we measure the gradients of Fe^{2+}, SO_4^{2-}, NO_3^-, NH_4^+, DOC, TC and TN in the pore water of the sediment, and combining the vertical distribution of the functional microorganisms involved in S, Fe and N cyclings in the sediments to determine the redox stratification in the sediment. It is found that the geochemical gradient of S, Fe and N of the reservoir sedimentary column is mainly defined by the redox process involved in the related functional microorganisms. According to the type of electron acceptor, the sediment profile is divided into 3 redox intervals, namely aerobic respiration (0–10 cm), denitrification/iron reduction (10–28 cm) and sulfate reduction (28–32 cm). In the aerobic respiration zone, NH_4^+ is oxidized by aerobic AOB to NO_3^- (0–5 cm), and Fe^{2+} is oxidized by microaerobic FeRB to Fe^{3+} (3–10 cm). In the denitrification/iron reduction zone, *Acinetobacter* and *Pseudomonas*, as the dominant NRB genera, may use nitrate as an electron acceptor to oxidize Fe^{2+} (11–16 cm). The dominant genera in SOB, such as *Sulfururvum*, *Thiobacillus* and *Thioalkalispira*, may use nitrate as an electron acceptor to oxidize sulfide, leading to SO_4^{2-} accumulation (14–24 cm). In the sulfate reduction zone, SO_4^{2-} is reduced by SRB. This study found that functional microorganisms forming comprehensive local ecological structures to adapt to changing geochemical conditions, and which would be potentially important for the degradation and preservation of C and the fate of many nutrients and contaminants in reservoirs.

Keywords Reservoir sediment · Geochemical cycle · Microbial community · Redox · Denitrification

1 Introduction

Reservoirs as an artificial ecosystem, their environmental impact and the possible material energy cycle process are fundamentally different from natural water ecosystems (Guo et al. 2021). The dam interrupts the continuity of natural water flow, resulting in a drop in water speed and an increase in water residence time, thereby promoting the accumulation of sediment (Rapin et al. 2020; Miranda et al. 2021). Reservoir sediments contain 25–30% of river sediment flux and play an important role in biogeochemical cycling (Vörösmarty et al. 2003). Furthermore, rising water levels alter the physical and chemical conditions of the sediment (such as dissolved oxygen, electron acceptors, organic matter, etc.), thus affects the biogeochemical cycle process in sediments (Eli 2008; Bryant, Little, and Helmut 2012).

In the absence of light at the bottom of the reservoir, the redox reaction is the only source of energy for microbial metabolism in the sediment (Barak et al. 2017). In the

✉ Xue-Ping Chen
xpchen@shu.edu.cn

✉ Fushun Wang
fswang@shu.edu.cn

[1] School of Environmental and Chemical Engineering, Shanghai University, 99 Shangda Road, BaoShan District, Shanghai 200444, China

[2] Department of Health and Environmental Sciences, Xi'an Jiaotong-Liverpool University, Suzhou 215123, Jiangsu, China

steady-state deposition system, aerobic respiration, denitrification, manganese (IV) reduction, iron (III) reduction, sulfate reduction and methane generation would occur in a thermodynamic sequence (Froelich et al. 1979). The redox chain, however, can overlap and even reverse due to the complex environment and components, such as the availability and reactivity of the electron acceptor (Barak et al. 2017). Continuously deposited organic materials in reservoir sediments would be partially recycled and converted into secondary substances, resulting in a zone of intense heterotrophic activity (Frascareli et al. 2019). This is anticipated that the microbial community actively participate in the material cycle, thereby forming a unique geochemical gradient in a reservoir (Chen et al. 2017; Wurzbacher et al. 2017).

In addition to the carbon cycle, the most important active redox cycles in freshwater sediments are the iron, nitrogen and sulfur cycles. Iron and sulfur-oxidizing bacteria have been shown to predominate in eutrophic freshwater sediments (Long et al. 2017). Iron oxidizing bacteria and sulfur-oxidizing bacteria oxidize ferrous and sulfide to Fe(III) and sulfate, respectively. In the study of Taihu Lake, it was found that three types of bacteria (*Sulfuricurvum*, *Sideroxydans*, and *Gallionella*) and one type of archaea (*Thermoplasmata*) related to iron and sulfur oxidation accounted for 43.4% and 38.4% of the total number of bacteria and archaea, respectively (Jiang et al. 2015). Ammonium can be converted to nitrite by ammonia-oxidizing bacteria in oxygen-permeated surface sediments, and then to nitrate through nitrification (Melton et al. 2014a, b). After the oxygen is depleted, the predominant redox mechanism is microbial metabolism with nitrate as the electron acceptor, and anaerobic oxidation of ferrous and sulfide occurs in the denitrification zone (Simone et al. 2001; Bosch et al. 2011). In deeper sediments, iron-reducing bacteria and sulfur-reducing bacteria are more abundant. Thermodynamically, the reduction of Fe(III) to ferrous is expected to be more advantageous than the reduction of sulfate to sulfide. As a result, it is believed that iron-reducing bacteria outperform sulfate-reducing microorganisms (Capua et al. 2019). However, with simultaneous iron and sulfate reduction, the dynamics of competition between microorganisms that govern iron and sulfate reduction have lately been reevaluated.

Determining the coupling between sulfur, iron and nitrogen cycles in reservoir sediments has important ecological significance because their vertical stratification affects sediment ecosystems. Compared with studies on water bodies, reservoir sediments have remained relatively unexplored to the biogeochemical cycles of sulfur, iron, and nitrogen coupling. Here we show how the bacterial distribution of the sulfur, iron and nitrogen cycles participates in the geochemical redox zone, where the sulfur, iron and nitrogen cycles overlap and how they affect one another. Therefore, the purpose of this study is to 1) quantify the important electron acceptors and donors in the sulfur, iron, and nitrogen cycles; 2) profile the vertical distribution of microbial community involved in S, Fe and N cyclings in the reservoir sediments; 3) identify the relationship between environmental factors and microbial groups involved in S, Fe and N cycling.

2 Materials and methods

2.1 Site description and sampling procedure

Hongfeng Reservoir is a eutrophic reservoir located in Guiyang City, Guizhou Province, southwestern China (106°19–106°28'E, 26°26'–26°35'N), with a humid subtropical monsoon climate. There is no severe heat in summer, no severe cold in winter, abundant rainfall and moderate sunshine. The annual average temperature is 14°C, the annual rainfall is between 1091.8 and 1414.5 mm, and the annual average sunshine is 100–150 h. There is plenty of rain in summer, with rainfall of ~ 500 mm. The night precipitation accounts for 70% of the annual precipitation, and the dry and wet seasons are not obvious. Hongfeng Lake Reservoir controls catchment water with an area of 1551 km^2, a storage capacity of 601 million cubic meters, a water surface area of 57.2 km^2, a maximum water depth of 45 m, and an average water depth of 10.5 m.

The sediment samples were taken in July 2019 in the middle of lacustrine in Hongfeng Reservoir (26°30'N, 106°25'E), where was 30 m water depth. The intact sediment core (38 cm) was collected through an open-ended sampling tube made of polymethyl methacrylate with an internal diameter of 6.0 cm and a length of 80 cm. The sediment core was segmented on site, and the depths of 0–20 cm were divided into 1 cm, while depths of 20–38 cm were divided into 2 cm, a total of 29 points. After that, pore water was extracted immediately by the Rhizon sampler from the segmented sediments and stored at 4 °C to determine the geochemical parameters. The solid samples were stored at − 20 °C for subsequent processing (DNA extraction and sequencing).

2.2 Geochemical analyses of pore water

The pore water samples were filtered with a 0.22 μm filter membrane before testing. Dissolved organic carbon (DOC) and Dissolved inorganic carbon (DIC) were measured by TC/TN analyzer (Multi N/C 3100, Jena, Germany). The Dissolved ferrous iron (Fe^{2+}) and ammonium salt (NH_4^+) were measured by spectrophotometer (Microplate reader,

Tecan, Switzerland) at wavelengths of 560 and 660 nm, respectively. NO_3^- and SO_4^{2-} were measured by ion chromatography (ICS-1100, Thermo, USA), the column of the detector was IonPac AG19-250/4.0 (Dionex, USA), and the flow rate was set as1.0 ml min^{-1}.

2.3 DNA extraction

Approximately 0.5 g sediment was extracted using the FastDNA SPIN Kit for Soil as directed by the manufacturer (MP Biomedicals, USA). Determine the concentration and quality of DNA by microvolume UV–Vis spectrophotometer (Q5000, Quawell, USA), and test the integrity of DNA by 1% (w/v) agarose gel electrophoresis (100 V, 30 min).

2.4 Illumina sequencing and analysis

Library preparation and sequencing were conducted by Majorbio, Inc (Shanghai, China) using the MiSeq Illumina platform. Primer pair 338F (5'-ACTCCTRCGGGAGG-CAGCAG-3') and 806R (5'-GGACTACCVGGGTATC-TAAT-3') were used to amplify the V3–V4 region of bacterial 16S rDNA. The PCR reaction system was carried out in a volume of 20 μL, which contained 4 μL of 5 × FastPfu buffer, 2.5 mM for each dNTPs, 2 pmol for each forward and reverse primer, 0.4 μL FastPfu polymerase, 0.2 μL BSA and ~ 10 ng of DNA template. The procedure of PCR cycle was as follows: 95 °C for 5 min, followed by 28–30 cycles of 94 °C for 10 s, 52–64 °C for 30 s and 72 °C for 30 s, and finally at 72 °C for 7 min.

The original sequence obtained by MiSeq sequencing were subjected to quality control filtering, and the inferior sequences were eliminated. Perform bioinformatics statistical analysis on OTUs at a similar level of 97% (version 7.0, http://drive5.com/uparse/). The ribosome database project (RDP) classifier (Cole et al., 2007) and the training set extracted from the Silva108 database (Quast et al., 2012) were used to classify the representative sequences of each OTU. For the results of OUT clustering and annotation analysis, further data analysis can be performed on Majorbio's I-Sanger platform (http://www.i-sanger.com/), which integrates various applications for microbial community analysis Software package. All sequences were submitted to the Sequence Read Archive under the BioProject accession numbers SAMN20370501 to SAMN20370529.

2.5 Statistical analyses

To explore the relationship between geochemical properties and microorganisms, Spearman analysis (SPSS 25.0, USA) was carried out. To study the co-occurrence mode among the redox-related functional genera of sulfur, iron and nitrogen, based on Spearman coefficient $R > 0.4$ and p-value < 0.01, the network diagram was drawn by Cytoscape software.

3 Result

3.1 Geochemical characterization of the sediment

The pore water was collected from the 38 cm sediment core and measured geochemical characterization at the 1 or 2 cm depth interval (Fig. 1). The concentration of DIC is higher than DOC in the upper (1–12 cm) and deeper sediment layers (22–38 cm), while in the middle sediment layers (13–20 cm), they were close to each other (Fig. 1a). The DOC concentration increased significantly from 1.8 to 5.1 mM at depth of 1–14 cm, after which the DOC concentration decreased slightly again to 2.5–3.4 mM below 26 cm depth. The major peak of DIC was found with a concentration of 6.8 mM at 8 cm depth. The Fe^{2+} concentration fluctuated between 0 and 0.2 mM at depth of 13–22 cm, which was obviously lower than upper (1–12 cm) and deeper sediment layers (24–38 cm) whose maximum concentration was 1.3 and 0.7 mM, respectively (Fig. 1b). Sulfate increased from 0.04 to 0.51 mM at depth of 8–22 cm and then dropped sharply to 0.5 mM at depth of 24 cm (Fig. 1c).

The nitrate concentration profile fluctuated between 10.0 and 12.9 μM, which was significantly lower than ammonium and the total nitrogen (TN) (Fig. 1d). The concentration of Ammonium increased significantly with increasing sediment depth of 1–8 cm, with a maximum concentration of 1.1 mM. Subsequently, Ammonium firstly dropped to 0.8 mM then lightly rose again to 1.1 mM at 18 cm depth then fluctuated between 0.8 and 1.0 mM (Fig. 1e). TN accumulated from 1.0 mM in the first cm of sediment to 2.8 mM at 14 cm depth, after which it fluctuated between 2.1 and 2.5 mM (Fig. 1f).

3.2 Diversity and relative abundance of sulfur, iron and nitrogen-metabolic microorganisms

The relative abundance of sulfur, iron and nitrogen-metabolic microorganisms at the genus level in the core of the sediment sample are summarized in Fig. 2, including sulfide oxidizing bacteria (SOB), sulfate-reducing bacteria (SRB), Fe oxidizing bacteria (FeOB), Fe reducing bacteria (FeRB), ammonia-oxidizing bacteria (AOB) and nitrate-reducing bacteria (NRB). The relative abundance of the above functional microorganisms was found accumulated in different sedimentary layers (Fig. 2a). In the surface sediment layer of 0–5 cm, AOB was much prevalent than

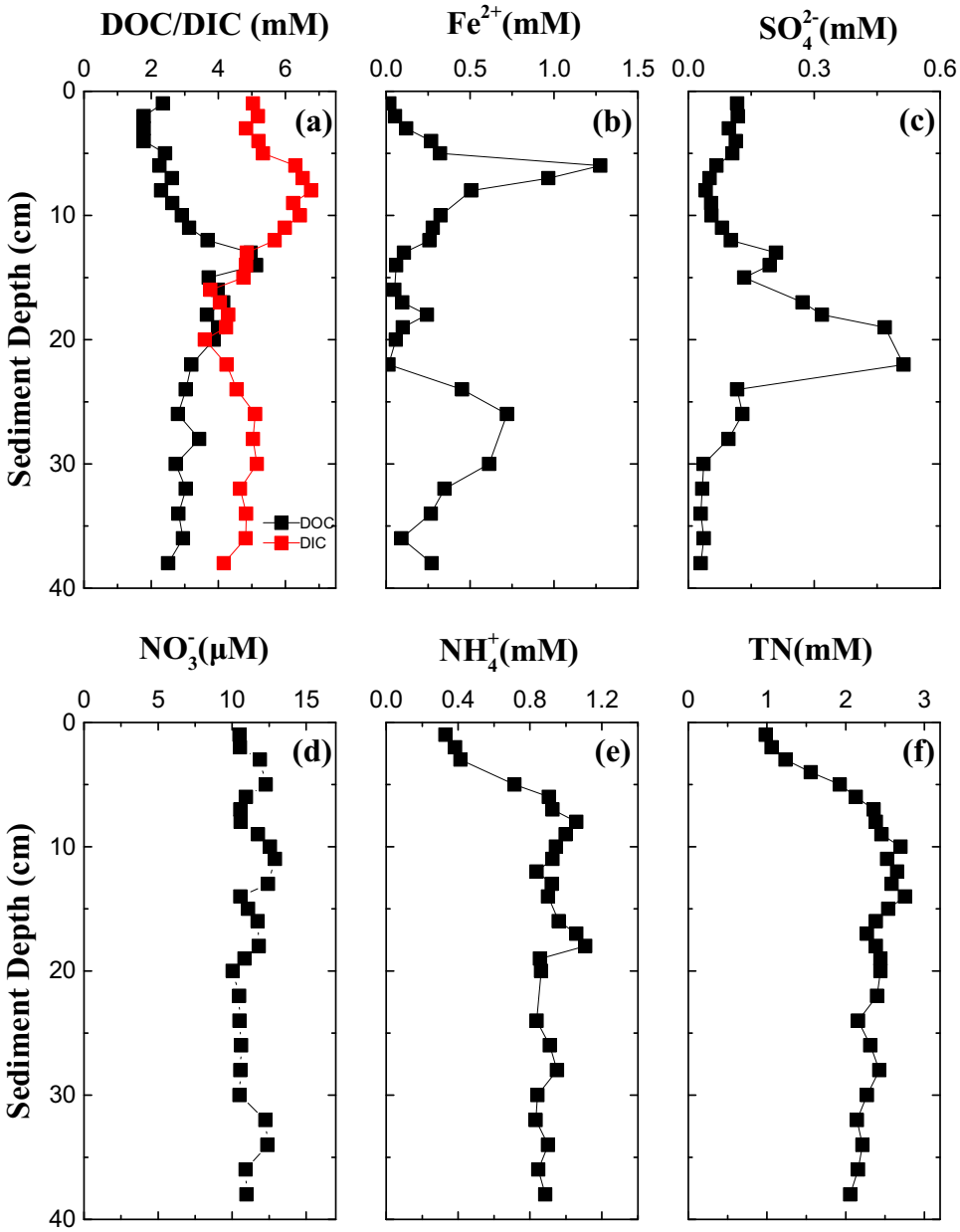

Fig. 1 Geochemical characteristics of the sediment. (a)DOC and DIC, (b)Ferrous ion (Fe^{2+}), (c)Sulfate (SO_4^{2-}), (d)Nitrate (NO_3^-), (e)Ammonium (NH_4^+), (f) Total dissolved nitrogen (TN)

other sediment layers, followed by FeOB which was significantly rich between 3 and 10 cm depth. In the middle sediment, SOB, FeRB and NRB all were more abundant than other sediment layers. NRB was found accumulated in the depth of 11–16 cm where would partially overlap with the rich space of FeRB and SOB. FeRB was enriched at the depth of 9–20 cm, while SOB extended to the deeper sediment (14–24 cm). In the deeper sediment layer, SRB lightly accumulated in the depth of 28–32 cm.

The relative abundance of SOB is significantly higher than SRB in all the sediment samples, and SOB was more than 70 times of SRB in the depth of 15–20 cm, although they had the same number of genera (Fig. 2b, c). A total of 7 genera, including *Sulfuricurvum*, *Thiobacillus*, *Thioalkalispira*, *Sulfurisoma*, etc. were confirmed as SOB (Fig. 2b). Among these genera, *Sulfuricurvum* and *Thiobacillus* together account for 13.9–64.4% of the total bacteria in all sediments samples, which also were the two most abundant genera of the total bacteria. And they reached the maximum peaks in the middle (15 cm, 50.9%) and deeper sediment layers (38 cm, 35.9%), respectively. Compared with *Sulfuricurvum* and *Thiobacillus*, the other subdivisions of SOB represented minor components. *Sulfurisoma* (0.26%), *Sulfuritalea* (0.48%) and *Sulfurimonas*

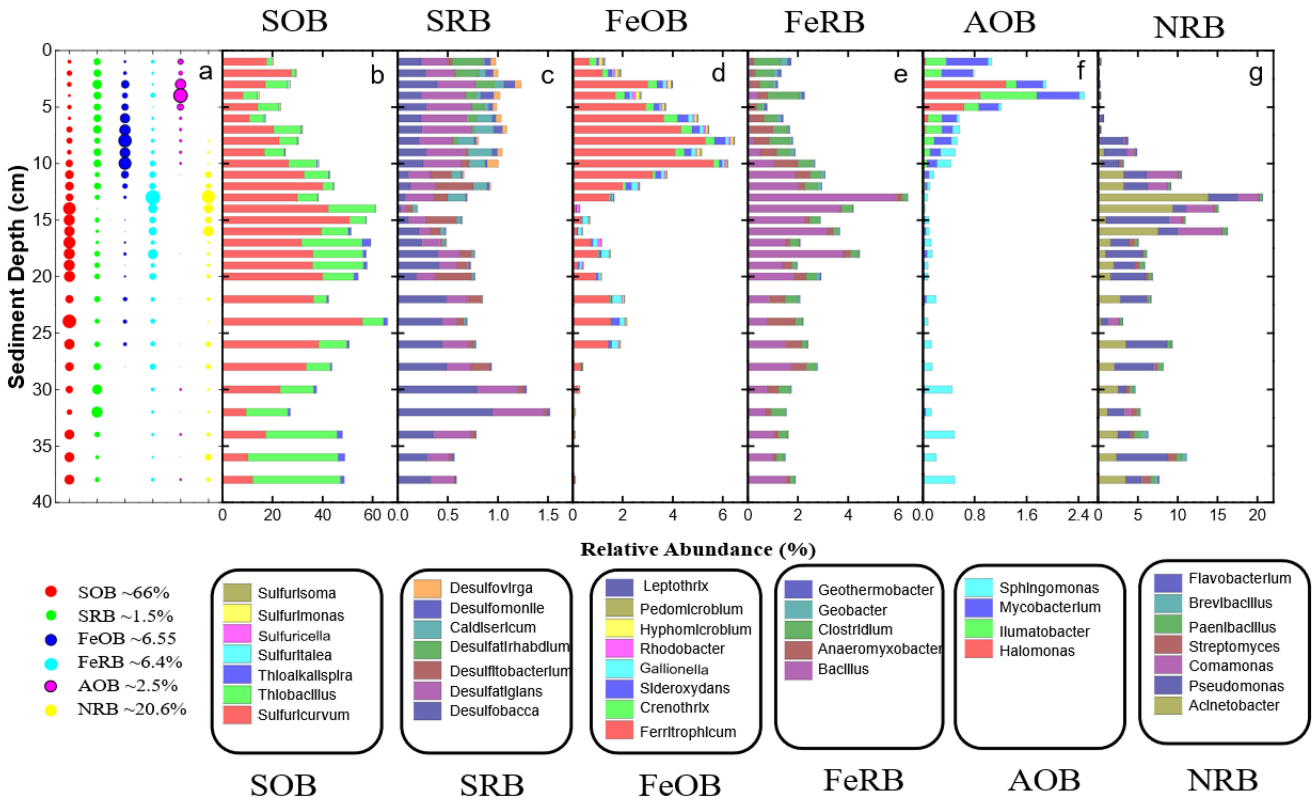

Fig. 2 Diversity of nitrogen, iron and sulfur-related metabolic microorganism of the sediment column profile. Putative sulfur iron and nitrogen metabolizing bacteria were identified based on phylogenetic affiliation with **a** the relative abundance of different functional microbial communities **b** sulfide oxidizing bacteria = SOB, **c** sulfur/sulfate-reducing bacteria = SRB, **d** Fe oxidizing bacteria = FOB, **e** Fe reducing bacteria = FeRB, **f** Ammonia oxidizing bacteria = AOB, and **g** Nitrate reducing bacteria = NRB

(0.30%) were equally reached peak in the surface sediment layer then steeply decreased to 0–0.04% below 10 cm depth. There were 7 genera, including *Desulfobacca Desulfatiglan Desulfatirhabdium*, etc., were classified as SRB (Fig. 2c). Among these genera, *Desulfobacca* and *Desulfatiglan* were the dominant genera of SRB, which were observed more abundant in sediment layers of 0–15 cm and 16–38 cm, respectively, with the maximum relative abundance 0.95% (32 cm) and 0.5% (7 cm). *Desulfatirhabdium* steeply decreased from 0.30% in the first cm of sediment to 0 below 9 cm depth.

The relative abundance of FeOB was higher than FeRB in the sediment of 1–12 cm depth, while in the deeper sediment of 12–38 cm depth, it was the opposite (Fig. 2d, e). Although 8 genera were numbers of putative FeOB, namely *Ferritrophicum Crenothrix*, *Sideroxydans,* etc., the relative abundances of them varied greatly (Fig. 2d). *Ferritrophicum* (maximum 5.6%, 10 cm) was the most prevalent genus of FeOB in all sediment samples, which was much higher than other subdivisions of FeOB and directly determined the changing trend of FeOB. The relative abundance of other subdivisions of FeOB, such as *Crenothrix* and *Hyphomicrobium*, was increased first then significantly decreased to 0.02% (15 cm), with the maximum relative abundance of 0.54% (6 cm) and 0.15% (4 cm), respectively. There were 8 genera were numbers of putative FeRB, including *Bacillus*, *Clostridium*, *Geothermobacter*, etc. (Fig. 2e). *Bacillus* as the most abundant genus of FeRB in sediment layers of 11–38 cm, increased significantly from 0.1% to 5.9% at depth of 1–13 cm, then decreased again to 0.8% in 22 cm depth, after which fluctuated between 0.8 and 1.8% in the depth of 22–38 cm. *Clostridium* dropped from 1.1% to 0.25% in the depth of 1–5 cm, then rose again to 0.84% at 8 cm, after which it fluctuated between 0.19 and 0.60% in the depth of 8–38 cm. *Geothermobacter* as the minor component of FeRB significantly drop from 0.14% to 0 in the depth of 1–13 cm, then fluctuated between 0 and 0.03% below 13 cm depth.

The relative abundance of NRB was 7–397 times of AOB in the sediment of 5–38 depth, while in the surface sediment of 0–5 cm depth, AOB was more abundant

(Fig. 2f, g). A total of 4 genera, including *Halomonas*, *Ilumatobacter*, *Mycobacterium* and *Sphingomonas* were confirmed as AOB (Fig. 2f). *Halomonas, Ilumatobacter* and *Mycobacterium* all were more abundant in the sediment layer of 0–11 cm depth, with the peak of 1.3% (3 cm), 0.87% (4 cm) and 0.65% (4 cm), respectively. Compared with the above genera, *Sphingomonas* as the least abundant genus of AOB was found in two major peaks at 9 cm (0.23%) and 38 cm (0.48%) depth. There were 8 genera were numbers of putative NRB, namely *Acinetobacter*, *Pseudomonas*, *Comamonas*, *Paenibacillus*, etc. (Fig. 2f). Among these genera, the relative abundance of *Acinetobacter* (0–0.03%), *Pseudomonas* (0.03–0.58%), *Comamonas* (0–0.04%) and *Paenibacillus* (0.01–0.03%) in the surface sediment of 1–7 cm all much lower than the deeper sediment, except for *Comamonas* which also hardly exists in the depth of 17–38 cm. In addition, *Acinetobacter*, *Pseudomonas* and *Paenibacillus* were found the major peak at 13 cm (13.8%), 15 cm (8.0%) and 36 cm (0.97%), respectively.

3.3 The correlations between geochemical factors and sulfur, iron and nitrogen -metabolic microorganisms

The correlations between geochemical factors and the relative abundance of functional microorganisms from sediment core (29 samples) were analyzed by Pearson correlation analysis (Figs. 1 and 4). DOC showed negative correlations with all of the genera of SRB (R = -0.62, $P < 0.01$), FeOB (R = -0.44, $P < 0.05$) and AOB (R = -0.70, $P < 0.01$) community, but a positive correlation with the genera of SOB (R = 0.69, $P < 0.01$), FeRB (R = 0.77, $P < 0.01$) and NRB (R = 0.79, $P < 0.01$) community (Figs. 2 and 4). DIC behaved oppositely for DOC, and it negatively correlated with *Thioalkaispira* (R = -0.55, $P < 0.01$), *Bacillus* (R = -0.38) and *Paenibacillus* (R = -0.52, $P < 0.01$) (Fig. 4). TN showed notable correlations with all genera of NRB and AOB community (Fig. 3), especially *Mycobacterium* (R = -0.82, $P < 0.01$) and *Pseudomonas* (R = -0.54, $P < 0.01$) (Fig. 4). In addition, TN was found a strong positive correlation with SOB (R = 0.54, $P < 0.01$), FeRB (R = 0.51, $P < 0.01$) (Fig. 3). NH_4^+ revealed the same trend of TN (Fig. 4). The depth distributions of Fe^{2+} significantly behaved positive correlations with all genera of FeOB, especially *Sideroxydans* (R = 0.53, $P < 0.01$), while a slight negative correlation with FeRB community which reflected by Bacillus (R = -0.32) (Fig. 4). Likewise, the depth distributions of SO_4^{2-} showed positive and negative correlations with SOB and SRB community respectively, which main reflected by *Sulfuricurvum* (R = 0.51, $P < 0.01$) and *Desulfatiglans* (R = -0.56, $P < 0.01$) (Fig. 4).

SOB community showed negative correlations with SRB (R = -−.52, $P < 0.01$), FeOB (R = -0.70, $P < 0.01$) and AOB (R = -0.70, $P < 0.01$), While positive with FeRB (R = 0.41, $P < 0.05$) and NRB (R = 0.54, $P < 0.01$) (Fig. 3). On the contrary, SRB community was found to negatively correlated with FeRB (R = -0.48, $P < 0.01$) and NRB (R = -0.62, $P < 0.01$) (Fig. 3). Except for sulfur-metabolic microorganisms, the FeRB also correlated with AOB (R = -0.41, $P < 0.05$) and NRB (R = 0.78, $P < 0.01$), while FeOB negative

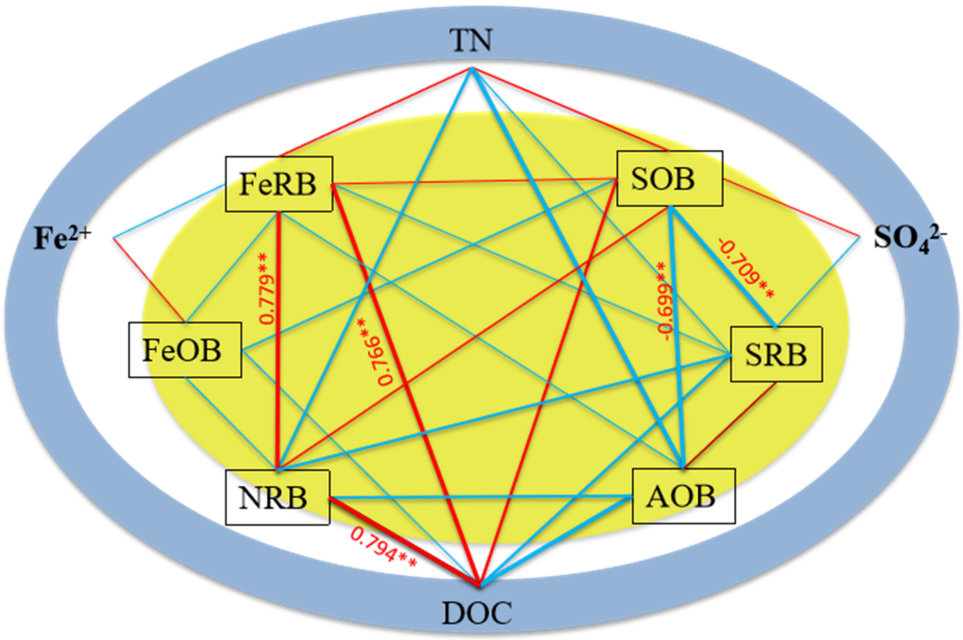

Fig. 3 Depict direct and indirect regulatory pathways of geochemical factors that affect the microbial community. The different shade areas represent the environmental factors (blue) and relative abundance of sulfur, iron and nitrogen-metabolic microorganisms (yellow), respectively. The lines represent positive (red) or negative (blue) path coefficients. The width of the line is proportional to the strength of the relationship. The number on the line is standardized direct path coefficients. * $p < 0.05$; ** $p < 0.01$ (n = 29)

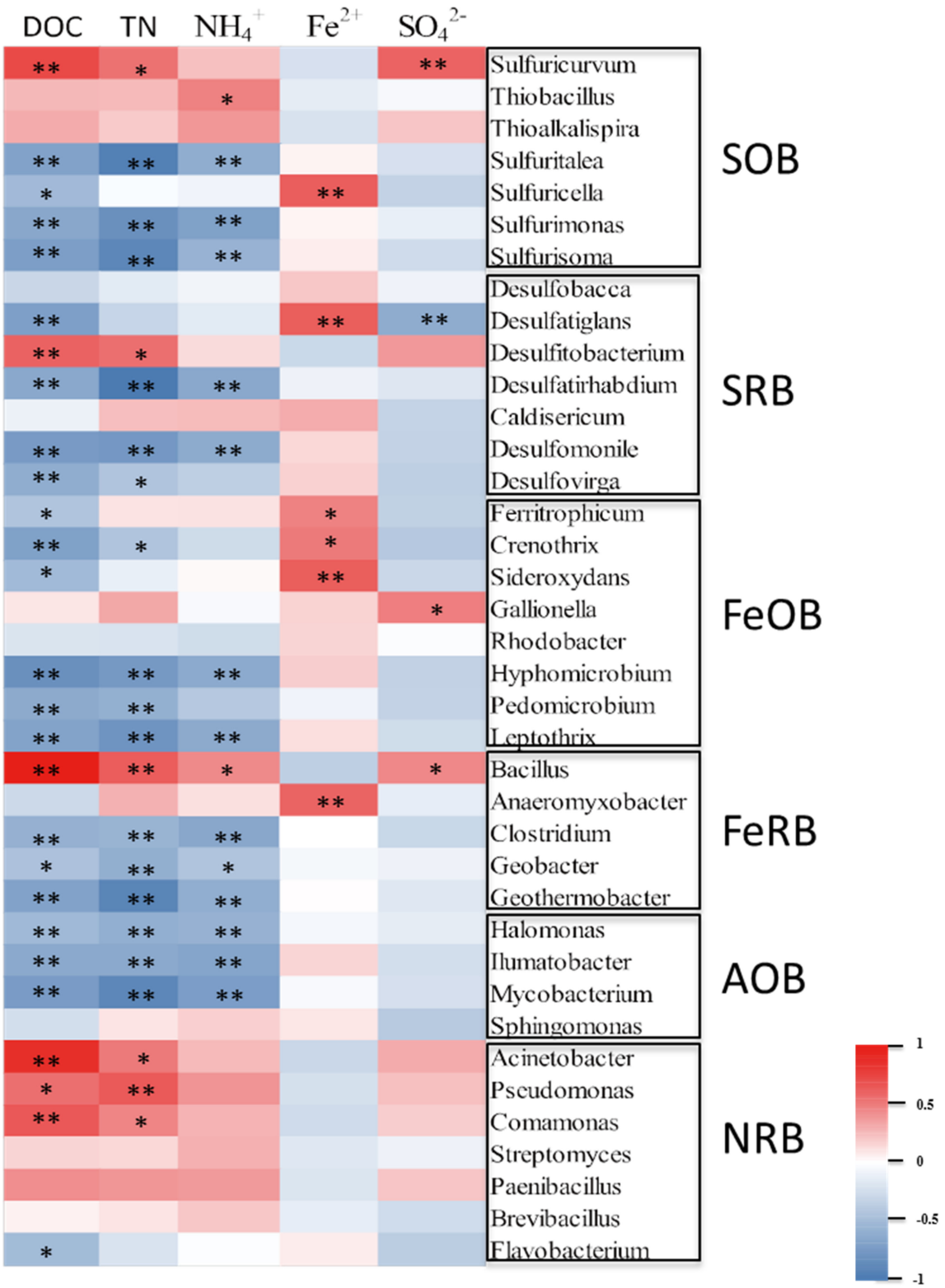

Fig. 4 The correlation analysis between geochemical properties and functional microbial groups, and the correlation R and P values are obtained through calculation. The legend on the right is the color interval for different R values. *, $p < 0.05$; **, $p < 0.01$ (n = 29)

correlations with NRB (R = − 0.45, $P < 0.05$) (Fig. 3). And AOB significantly correlated with NRB (R = − 0.64, $P < 0.01$) (Fig. 3).

3.4 Network analysis of microbial co-occurrence patterns involved in iron, nitrogen and sulfur cycles

The coupling processes of different microbial functional genera involved in iron, nitrogen and sulfur metabolism were explored in co-occurrence analysis. Those functional genera were found to have strong connectivity with each other, and the network of them has 35 nodes and 240 edges, of which 76 were positively connected and 164 were negatively connected (Fig. 5). The genera of iron-metabolic microorganisms as the critical nodes, such as *Crenothrix*, *Hyphomicrobium*, *Geothemobacter*, etc., was notably correlated with other functional genera (Fig. 5). *Crenothrix* and *Hyphomicrobium*, the two most prevalent FeOB groups, embraced positive correlations with the genera of SRB (R > 0.56, $P < 0.01$) and AOB (R > 0.48, $P < 0.01$) in the network, while negative correlations with the genera of NRB (R < − 0.51, $P < 0.01$), except for *Flavobacterium* (Fig. 5). The nitrogen-metabolic microorganisms also were found to have the essential nodes namely *Paenibacillus* and *Mycobacterium*, and they showed opposite connections with other functional genera (Fig. 5). *Paenibacillus* of NRB possessed 17 edges negatively connected with other functional genera (R < − 0.53, $P < 0.01$), while only 2 edges positively connected with *Thiobacillus* (R = 0.70, $P < 0.01$) and *Thioalkalispira* (R = 0.73, $P < 0.01$) of SOB (Fig. 5). On the opposite, *Mycobacterium* of AOB embraced 15 edges positive connection with other functional genera (R > 0.61, $P < 0.01$), except for *Thiobacillus*, *Thioalkalispira* and *Thioalkalispira* of SOB and *Bacillus* of FeRB (Fig. 5). As for the genera of sulfur-metabolic microorganisms, such as *Sulfurisoma*, *Desulfomonile*, *Desulfovirga*, etc., they were less important than functional genera involved in iron and nitrogen (Fig. 5).

4 Discussion

4.1 Coupling of sulfur, iron, and nitrogen cycle processes in the denitrification zone

The distribution of a series of functional species in the denitrification sedimentary layer is unexpectedly comparable, which triggers the thinking of the element cycle coupling mechanism. Among these SOB taxa, *Sulfuricurvum*, *Thiobacillus* and *Thioalkalispira* were thought to be autotrophic denitrifying bacteria capable of nitrate-reduced sulfide oxidation (Pokorna and Zabranska 2015; Shao et al. 2010). *Thiobacillus*, in particular, may oxidize not only sulfur compounds but also ferrous, even insoluble FeS and Fe (Haaijer et al. 2007; Hayakawa et al. 2013). *Sulfuricurvum* had no significant connections with *Thiobacillus* or *Thioalkalispira*, while *Thiobacillus* was significantly

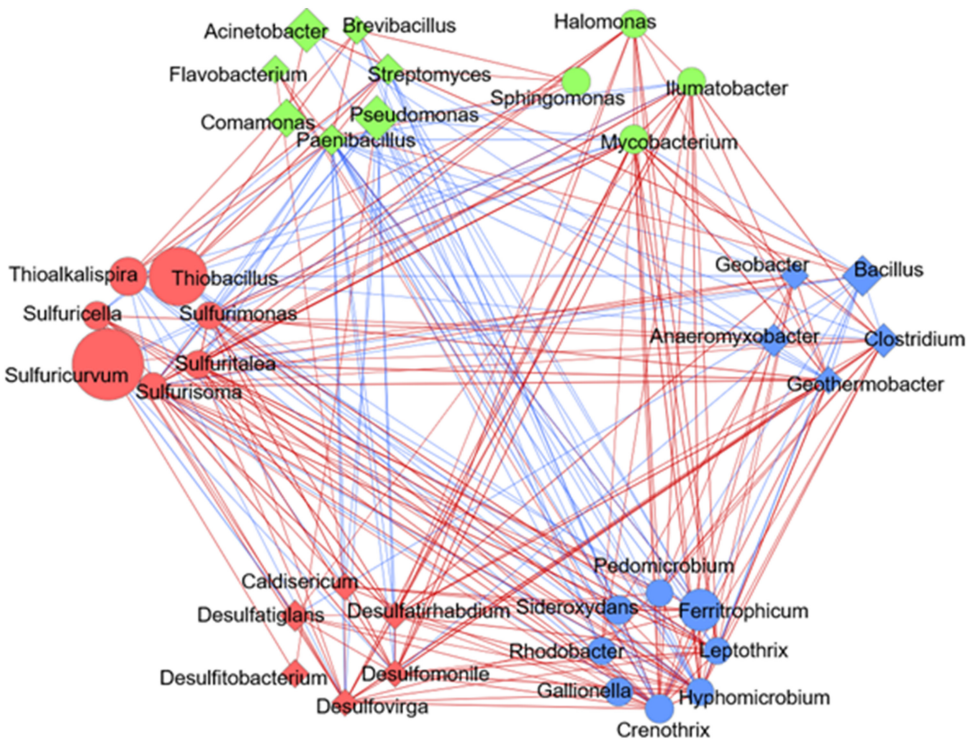

Fig. 5 Network analysis of co-occurring microbial functional genera in sediments (Spearman, R > 0.4, $p < 0.01$). Different functional genera are marked with different shapes (circles are oxidizing bacteria, triangles are reducing bacteria) and color (red are sulfur functional bacteria, blue are iron functional bacteria, and green are nitrogen functional bacteria). The size of each node is proportional to the number of connections

correlated (R = 0.77, $P < 0.05$) with *Thioalkalispira*. These chemoautotrophic denitrifying bacteria were common in the denitrification interval (13.9%-65.8%), showing that autotrophic denitrification is the primary nitrogen pathway in Hongfeng Reservoir (Jiang et al. 2015). However, the heterotrophic cannot be overlooked. NRB genera *Acinetobacter*, *Pseudomonas*, and *Comamonas* were thought to be heterotrophic denitrifying bacteria capable of nitrate-reduced ferrous oxidation (Kiskira et al. 2016). These three taxa were all strongly positively correlated with *Bacillus* ($R > 0.46$, $P < 0.05$), explaining why ferrous did not accumulate during the denitrification interval.

$$FeS_2 + 3NO_3^- + 2H_2OFe(OH)_3 + 2\ SO_4^{2-} + 1.5N_2 + H^+ \quad (1)$$

$$5\ FeS_2 + 14NO_3^- + 4H^+ 5\ Fe^{2+} + 7N_2 + 10\ SO_4^{2-} + 2\ H_2O \quad (2)$$

$$2\ NO_3^- + 10\ Fe^{2+} + 12H^+ N_2 + 10\ Fe^{3+} + 6\ H_2O \quad (3)$$

NO_3^- reduction to NO_2^- may also occur as follows:

$$2\ FeS_2 + 15NO_3^- + 7\ H_2O2\ Fe(OH)_3 + 15NO_2^- + 4SO_4^{2-} + 8\ H^+ \quad (4)$$

High quantities of ferrous iron and sulfate were found in the pore water of Hongfeng Reservoir. As a result, sediments may be rich in quickly oxidized metal sulfides (FeS_2), which are highly absorbable by microorganisms (Haaijer et al. 2008). Anaerobic oxidation of pyrite should be thermodynamically feasible, requiring electron acceptors with positive redox potential, such as nitrate (Eq. 1). In terms of energy savings, sulfur reduction outperforms iron reduction. As a result, sulfur will be preferentially oxidized to sulfate, whereas ferrous iron will be eluted (Eq. 2) (Capua et al. 2019) and oxidized to ferric iron if nitrate is sufficient (Eq. 3). nitrite will accumulate if nitrate reduction is insufficient. In this case, the reaction followed the steps shown in Eq. 4 (Bosch et al. 2011). Because the overall nitrogen and ammonia levels in the pore water were stable, it was assumed that nitrate might be converted to nitrite during the denitrification interval. This process may prevent nitrogen in the sediments from being lost as gaseous nitrogen as a result of complete denitrification, resulting in nitrogen accumulation in the sediments. As a result, soluble nitrogen-containing compounds were continually released from the sediment into the water, accelerating eutrophication in the Hongfeng Reservoir.

4.2 Factors driving the stratification of geochemical gradient of S, Fe and N

Based on the redox "tower" of microorganisms, aerobic respiration, denitrification (Otte et al. 2018), Mn(IV) reduction, Fe(III) reduction and sulfate reduction occur in the order of thermodynamics, generating a typical geochemical gradient (Orcutt et al. 2011; Schink 2010). Most microorganisms' vertical distribution in our study region was related to geochemical gradients, particularly sulfur, iron, and nitrogen-metabolic bacteria (Fig. 3). Assuming that the above three species of functional microorganisms thrived in the Hongfeng reservoir, their niches should have followed the gradient of the redox tower and accumulated at various depths. Indeed, the sediments in our study area were divided into three redox intervals based on the electron acceptor type, namely aerobic respiration, denitrification/iron reduction and sulfate reduction (Fig. 6). In addition to the impacts of thermodynamic gradients, kinetics, substrates, electron acceptor availability and even competition may directly limit the niche of microbes (Melton et al. 2014a, b; Laufer and Katja 2016). Aerobic respiration was carried out by microorganisms in the oxygen-permeable sedimentary layer. Aerobic AOB accumulated preferentially in the depth of oxygen-rich sediment, whereas FeOB subsequently appeared in slightly deeper micro-oxygen sediment (Widdel et al. 1993). Although the microbial oxidation of ferrous iron was thermodynamically beneficial, it was nevertheless kinetically constrained (Custer 1983). The surface sediment was oxygen-rich, where chemical iron oxidation takes precedence over biological iron oxidation. (Druschel et al. 2008). As oxygen was consumed throughout the depths, the chemical reaction kinetics decreased substantially, resulting in microaerobic FeOB aggregating (Vollrath et al. 2012). Denitrification with nitrate as the electron acceptor became the predominant microbial process in the oxygen-depleted sedimentary layer, where NRB is predominant (Jetten 2008). More than 94% of SOB, notably *Sulfuricurvum, Thiobacillus*, and *Thioalkalispira*, were capable of coupling nitrate reduction and sulfide oxidation (Haaijer et al. 2007). These genera were found in the same sedimentary layer as NRB and were significantly connected with it (R = 0.54, $P < 0.01$). FeRB, which should accumulate in deeper layers, was particularly abundant in the denitrification period, demonstrating a substantial association with NRB (R = 0.78, $P < 0.01$). This could be owing to the denitrification of NRB to form ferric iron, which provided FeRB with an available electron acceptor. SRB followed the redox gradient at the bottom of the sediments and accumulated somewhat deeper than the aerobic respiration, denitrification and iron reduction layers.

The metabolic processes of the functioning microorganisms indicated above in their habitats have also generated a typical geochemical gradient. Ammonium was oxidized to nitrate by aerobic AOB at the surface sedimentary layer of aerobic respiration. As the depth increased, oxygen was gradually depleted, AOB nearly

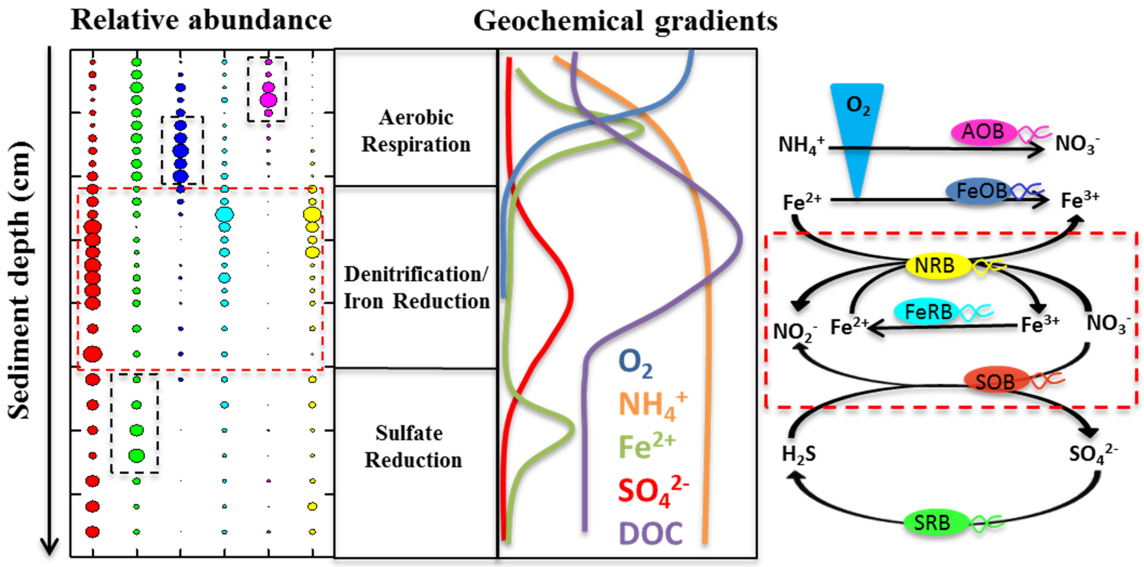

Fig. 6 Niche partition of functional genera involved in iron, nitrogen and sulfur along geochemical gradients

vanished, and ammonium accumulated. AOB was strongly inversely associated with ammonium ($R = -0.65$, $P < 0.01$). In oxygen-rich sediment, chemical ferrous oxidation occurred and ferrous accumulated as the oxygen content declined. When the oxygen level reached a threshold point, the microaerobic FeOB gathered swiftly to oxidize ferrous, demonstrating a substantial positive correlation with ferrous ($R = 0.42$, $P < 0.05$). The abundant genera *Acinetobacter*, *Pseudomonas*, and *Comamonas* of NRB have the potential to connect nitrate reduction and iron oxidation in the sedimentary layer of denitrification. However, these three NRB genera, as well as all FeRB genera, were not significantly connected to Ferrous ion. The balance between continuous oxidation and reduction may cause the decoupling of iron-functional bacteria from the geochemical gradient in the denitrification area (Kappler and Bryce 2017). FeRB reduced Fe(III) produced by denitrification to ferrous, which was then rapidly oxidized to Fe(III) by denitrification, resulting in ferrous in a low concentration steady state. The dominant genus *Sulfuricurvum* of SOB may have conducted nitrate reduction and sulfide oxidation processes, resulting in sulfate accumulation in this interval. *Sulfuricurvum* was found to have a substantial positive correlation with sulfate ($R = 0.51$, $P < 0.01$). Organic matter was oxidized and degraded in the sulfur-reduced sedimentary layer, and SRB was strongly inversely linked with DOC ($R = -0.62$, $P < 0.01$).

4.3 Environment impact on the geochemical gradient in the reservoir sediment

Sediment serves as a reservoir for nutrients in the aquatic ecosystem, particularly nitrogen, iron and sulfur, which are essential components of living creatures and have a significant effect on the aquatic ecosystem's biological environment. Low dissolved oxygen levels in the reservoir due to seasonal temperature stratification altered metabolic processes and material movement in the sediments. Additionally, oxygen exposure in these sediments has a direct effect on the preservation of sedimentary organic carbon, and bottom water anoxia improves carbon burial effectiveness (Friese et al. 2021). Iron is a typical redox-active element, and iron oxidation may drive primary productivity and nutrient cycling in dark settings such as deep reservoirs (McAllister et al. 2020). The sulfur reduction affects metal circulation and bioavailability, and the S2- content in sediment profiles is a critical factor regulating the availability and toxicity of metal elements (Toro et al. 1992). The connection of iron and sulfur is critical for the biogeochemical transformation and circulation of endogenous phosphorus in reservoirs (Rozan et al. 2002). The distribution of Fe and S system occurrence forms and their coupling relationship reveals the sediment geochemical gradient distribution, providing a scientific foundation for understanding reservoir sedimentary evolution and water quality management.

5 Conclusion

In the reservoir sedimentary, the geochemical gradients of S, Fe and N are mainly defined by the redox process involved in their related functional microorganisms. According to the type of electron acceptor, the sedimentary column profile is divided into 3 redox intervals, namely aerobic respiration, denitrification/iron reduction and sulfate reduction. The distribution of a series of functional species in the denitrification sediments is unexpectedly comparable, indicating that there are obvious element coupling reactions in this area, including the coupling of denitrification and iron oxidation by NRB, and the coupling of denitrification and sulfide oxidation by SOB. In addition, the abundant presence of autotrophic denitrifying bacteria such as *Sulfuricurvum*, *Thiobacillus* and *Thioalkalispira* indicates that autotrophic denitrification is the main nitrogen conversion pathway in Hongfeng Reservoir. The accumulation of ammonia nitrogen and nitrate nitrogen in the pore water of the denitrification zone would prevent the nitrogen in the sediment from being lost in a gaseous manner through complete denitrification. The continuous release of soluble nitrogen compounds into the water body has aggravated the eutrophication of the Hongfeng Reservoir.

Acknowledgements This work was sponsored by National Key Research and Development Project by MOST of China (grant No. 2016YFA0601003) and Shanghai Science and Technology Development Foundation (No. 19010500100).

Declarations

Conflict of interest On behalf of all authors, the corresponding author states that there is no conflict of interest.

References

Blonder B, Boyko V, Turchyn AV , Antler G, Sinichkin U, Knossow N , Klein R, Kamyshny A (2017) Impact of aeolian dry deposition of reactive iron minerals on sulfur cycling in sediments of the Gulf of Aqaba. Front Microbiol 8:1131

Bosch J, Lee KY, Jordan G, Kim KW, Meckenstock RU (2011) Anaerobic, nitrate-dependent oxidation of pyrite nanoparticles by thiobacillus denitrificans. Environ Sci Technol 46:2095–2101

Bryant LD, Little JC, Burgmann H (2012) Response of sediment microbial community structure in a freshwater reservoir to manipulations in oxygen availability. Fems Microbiol Ecol 80:248–263

Chen J, Hanke A, Tegetmeyer HE, Kattelmann I, Sharma R, Hamann E, Hargesheimer T, Kraft B, Lenk S, Geelhoed JS (2017) Impacts of chemical gradients on microbial community structure. ISME J 11:920–931

Cole JR, Chai B, Farris RJ, Wang Q, Kulam-Syed-Mohideen AS, McGarrell DM, Bandela AM, Cardenas E, Garrity GM, Tiedje JM (2007) The ribosomal database project (RDP-II): introducing my RDP space and quality controlled public data. Nucleic Acids Res 35:169–172

Custer L (1983) The kinetics of the oxidation of ferrous iron in synthetic and natural waters. Geochim Cosmochim Acta 47:67–79

Di Capua FD, Pirozzi F, Lens PNL, Esposito G (2019) Electron donors for autotrophic denitrification. Chem Eng J 362:922–937

Druschel GK, Emerson D, Sutka R, Suchecki P, Iii G (2008) Low-oxygen and chemical kinetic constraints on the geochemical niche of neutrophilic iron(II) oxidizing microorganisms. Geochim Cosmochim Acta 72:3358–3370

Eli E (2008) Effects of thermal stratification and mixing on reservoir water quality. Limnology 9:135–142

Frascareli D, Gontijo ES, Melo S, Simonetti VC, Friese K (2019) Source of organic matter and flux studies of nutrients in a tropical reservoir of Brazil (Itupararanga dam, Sao Paulo state). Geophys Res 21:EGU2019-8823-1

Friese A, Bauer K, Glombitza C, Ordoñez L, Ariztegui D, Heuer VB, Vuillemin A, Henny C, Nomosatryo S, Simister R, Wagner D, Bijaksana S, Vogel H, Melles M, Russell JM, Crowe SA, Kallmeyer J (2021) Organic matter mineralization in modern and ancient ferruginous sediments. Nat Commun 12:2216

Froelich PN, Klinkhammer GP, Bender ML, Luedtke NA, Heath GR, Cullen D, Dauphin P, Hammond D, Hartman B, Maynard V (1979) Early oxidation of organic matter in pelagic sediments of the eastern equatorial Atlantic: suboxic diagenesis. Geochim Cosmochim Acta 43:1075–1090

Guo ZF, Boeing WJ, Borgomeo E, Xu Y, Weng YY, Weng Y (2021) Linking reservoir ecosystems research to the sustainable development goals. Sci Total Environ 781:146769

Haaijer S, Harhangi HR, Meijerink BB, Strous M, Pol A, Ajp Smolders K, Verwegen MJ, Op D (2008) Bacteria associated with iron seeps in a sulfur-rich, neutral pH, freshwater ecosystem. ISME J 2:1231–1242

Haaijer S, Lamers L, Smolders A, Jetten M, Op D (2007) Iron sulfide and pyrite as potential electron donors for microbial nitrate reduction in freshwater Wetlands. Geomicrobiol J 24:391–401

Hayakawa A, Hatakeyama M, Asano R, Ishikawa Y, Hidaka S (2013) Nitrate reduction coupled with pyrite oxidation in the surface sediments of a sulfide-rich ecosystem. J Geophys Res Biogeosci 118:639–649

Jetten M (2008) The microbial nitrogen cycle. Environ Microbiol 10:2903–2909

Chen N, Yang JS, Qu JH, Li HF, Liu WJ, Li BZ, Wang ET, Yuan HL (2015) Sediment prokaryote communities in different sites of eutrophic Lake Taihu and their interactions with environmental factors. World J Microbiol Biotechnol 31:886–896

Kappler A, Bryce C (2017) Cryptic biogeochemical cycles: unravelling hidden redox reactions. Environ Microbiol 19:842–846

Kiskira K, Papirio S, Van Hullebusch ED, Esposito G (2016) Fe(II)-mediated autotrophic denitrification: a new bioprocess for iron bioprecipitation/biorecovery and simultaneous treatment of nitrate-containing wastewaters. Int Biodeterior Biodegrad 119:631–648

Laufer K (2016) Abundance, distribution, and activity of anaerobic and microaerophilic Fe(II)-oxidizing and anaerobic Fe(III)-reducing microorganisms in coastal marine sediments. Dissertation of University of Tuebingen

Long J, Chang SL, Ahn CY, Lee HG, Lee S, Shin HH, Lim D, Oh HM (2017) Abundant iron and sulfur oxidizers in the stratified sediment of a eutrophic freshwater reservoir with annual cyanobacterial blooms. Sci Rep 7:43814

McAllister SM, Vandzura R, Keffer JL, Polson SW, Chan CS (2020) Aerobic and anaerobic iron oxidizers together drive denitrification and carbon cycling at marine iron-rich hydrothermal vents. ISME J 15:1271–1286

Melton ED, Behrens S, Kappler A, Schmidt C (2014a) High spatial resolution of distribution and interconnections between Fe- and N-redox processes in profundal lake sediments. Environ Microbiol 16:3287–3303

Melton ED, Stief P, Behrens S, Kappler A, Schmidt C (2014b) High spatial resolution of distribution and interconnections between Fe- and N-redox processes in profundal lake sediments. Environ Microbiol 16:3287–3303

Miranda MN, Rosa C, Peres A, Maia R (2021) Sedimentation assessment and effects in Venda Nova dam reservoir (Portugal). Sci Total Environ 766:144261

Orcutt BN, Sylvan JB, Knab NJ, Edwards KJ (2011) Microbial ecology of the dark ocean above, at, and below the seafloor. Microbiol Mol Biol Rev 75:361–422

Otte JM, Harter J, Laufer K, Blackwell N, Straub D, Kappler A, Kleindienst S (2018) The distribution of active iron-cycling bacteria in marine and freshwater sediments is decoupled from geochemical gradients. Environ Microbiol 20:2483–2499

Pokorna D, Zabranska J (2015) Sulfur-oxidizing bacteria in environmental technology. Biotechnol Adv 33:1246–1259

Quast C, Pruesse E, Yilmaz P, Gerken J, Schweer T, Yarza P (2013) The silva ribosomal rna gene database project: improved data processing and web-based tools. Nucleic Acids Res 41:590–596

Rapin A, Rabiet M, Mourier B, Grybos M, Deluchat V (2020) Sedimentary phosphorus accumulation and distribution in the continuum of three cascade dams (Creuse River, France)'. Environ Sci Pollut Res 27:6526–6539

Rozan T, Taillefert M, Trouwborst R, Glazer B, Ma S, Herszage J, Valdes L, Luther G (2002) Iron-sulfur-phosphorus cycling in the sediments of a shallow coastal bay: implications for sediment nutrient release and benthic macroalgal blooms. Limnol Oceanogr 47:1346–1354

Schink B (2010) Microbially driven redox reactions in anoxic environments: pathways, energetics, and biochemical consequences. Eng Life Sci 6:228–233

Shao MF, Tong Z, Fa Ng HP (2010) Sulfur-driven autotrophic denitrification: Diversity, biochemistry, and engineering applications. Appl Microbiol Biotechnol 88:1027–1042

Hauck S, Benz M, BruneSchink AB (2001) Ferrous iron oxidation by denitrifying bacteria in profundal sediments of a deep lake (Lake Constance). FEMS Microbiol Ecol 37:127–134

Toro DMD, Mahony JD, Hansen DJ, Scott KJ, Carlson AR (1992) Acid volatile sulfide predicts the acute toxicity of cadmium and nickel in sediments. Environ Sci Technol 26:96–101

Vollrath S, Behrends T, Van Cappellen P (2012) Oxygen dependency of neutrophilic Fe(II) oxidation by leptothrix differs from abiotic reaction. Geomicrobiol J 29:550–560

Vörösmarty CJ, Meybeck M, Fekete B, Sharma K, Green P, Syvitski JPM (2003) Anthropogenic sediment retention: major global impact from registered river impoundments. Global Planet Change 39:169–190

Widdel F, Schnell S, Heising S, Ehrenreich A, Assmus B, Schink B (1993) Ferrous iron oxidation by anoxygenic phototrophic bacteria. Nature 362:834–836

Wurzbacher C, Fuchs A, Attermeyer K, Frindte K, Grossart HP, Hupfer M, Casper P, Monaghan MT (2017) Shifts among eukaryota bacteria, and archaea define the vertical organization of a lake sediment. Microbiome 5:1–16